

# Non-Newtonian Stagnant Lid Convection and Magmatic Resurfacing on Venus

C. C. Reese and V. S. Solomatov

*Department of Physics, New Mexico State University, Las Cruces, New Mexico 88003*

E-mail: creese@nmsu.edu

and

L.-N. Moresi

*Australian Geodynamics Cooperative Research Centre, CSIRO Exploration and Mining, 39 Fairway, Nedlands 6009, Western Australia, Australia*

Received March 9, 1998; revised July 24, 1998

Mantle convection on Venus is likely to occur in the regime known as stagnant lid convection. We investigate this regime for internally heated convection with temperature- and pressure-dependent power-law viscosity (dislocation creep). Scaling relationships obtained for large aspect ratio convection are different from steady-state square box calculations but agree well with scaling theory and boundary layer stability analysis. Results for Arrhenius viscosity and pressure dependent viscosity show that the efficiency of heat transport is sensitive to the viscosity function at the bottom of the lid. New scaling relationships are applied to parameterized convection calculations of the thermal history of Venus assuming that plate tectonics could not occur during evolution. The onset of convection beneath the lid is delayed even for initial potential temperatures near the solidus. During the conductive regime, melting is suppressed due to the development of a thick cold lid at the surface. After convection begins, the lid becomes thinner and the planet undergoes a period of widespread melting and volcanism. The timing of the beginning and ending of melting depends on various factors such as the initial conditions and mantle rheology. The episode of melting predicted by the models can be reconciled with the cessation of global resurfacing on Venus 300–800 Myr ago. The models yield present-day lithospheric thicknesses around 200 km which is similar to previously suggested estimates. © 1999 Academic Press

**Key Words:** mantle convection; Venus; melting; non-Newtonian viscosity.

## INTRODUCTION

The efficiency of convective heat transport in the mantles of the terrestrial planets determines thermal history, volcanic and tectonic evolution, chemical differentiation, magnetic field history, and the present-day state including topography and gravity (McKenzie and Weiss 1975, Turcotte *et al.* 1979, Schubert *et al.* 1979, Sharpe and Peltier 1979, Stevenson and Turner 1979, Phillips *et al.* 1981, Cook and Turcotte 1981, Spohn

and Schubert 1982, Stevenson *et al.* 1983, Arkani-Hamed and Toksöz 1984, Christensen 1985a, Kaula 1990a,b, Phillips 1990, Phillips and Grimm 1990, Spohn 1991, Parmentier and Hess 1992, Zharkov and Solomatov 1992, Phillips and Hansen 1994, Solomatov and Moresi 1996, Nimmo and McKenzie 1996, Schubert *et al.* 1997).

Early studies of the efficiency of heat transport assumed constant or weakly variable viscosity convection (e.g., Turcotte and Oxburgh 1967, Moore and Weiss 1973, Jarvis and Peltier 1982, Christensen 1984, Christensen 1985a). However, strongly variable viscosity changes the convective style to the regime called stagnant lid convection for which the scaling relationships are entirely different (Morris and Canright 1984, Fowler 1985, Ogawa *et al.* 1991, Davaille and Jaupart 1993, Solomatov 1995, Moresi and Solomatov 1995, Doin *et al.* 1997, Trompert and Hansen 1998, Grasset and Parmentier 1998). This regime is characterized by the formation of a nearly immobile lid on top of the convective mantle due to the large viscosity of the upper thermal boundary layer.

Stagnant lid convection seems to be the appropriate convective regime on all the terrestrial planets except Earth. Earth appears to be a very special case—probably because of water (e.g., Kaula 1990a,b). Based on a comparison between convective planforms and topography, Schubert *et al.* (1997) suggested that Venus may be in the “sluggish lid” or transitional regime (Solomatov 1993, 1995). Although this is a possibility, for non-Newtonian viscosity, this style of convection exists only in a very narrow parameter range (Solomatov 1995, Solomatov and Moresi 1997). Additionally, heat is transported in this regime by lithospheric recycling and one would expect to find surface manifestations of plate motions which is not observed on Venus except in a few regions (Schubert and Sandwell 1995). Therefore, we concentrate our efforts on stagnant lid convection.

The most pronounced consequence of stagnant lid convection with temperature-dependent viscosity is substantially higher

mantle temperatures. Although melting always seemed to be an important factor in planetary evolution (e.g., Cook and Turcotte 1981, Spohn 1991, Zharkov and Solomatov 1992, Schubert *et al.* 1992), its degree and consequences were uncertain since it was not clear how high the absolute temperature of the planet might become. For temperature-dependent Newtonian viscosity (diffusion creep) the difference is many hundreds of degrees (e.g., Schubert *et al.* 1997). We can also look at this issue from another point of view: present-day Earth, which has a very efficient mechanism of heat transport, plate tectonics, is already close to the solidus. In the absence of plate tectonics, the mantle should be much hotter in order to remove the amount of heat corresponding to the present day heat flux. A similar conclusion was reached for non-Newtonian viscosity as well (Reese *et al.* 1998). However, these estimates were done on the basis of convection in a  $1 \times 1$  box which imposes artificial constraints on the flow and affects the scaling relationships. Also, the effect of pressure could not be accurately estimated in earlier models.

In this study we determine the efficiency of convective heat transport for temperature and pressure dependent non-Newtonian viscosity convection in an internally heated box with a large aspect ratio ( $4 \times 1$ ) and compare the results with previously suggested scaling relationships. Then we use the new scaling relationships to calculate the thermal and magmatic evolution of Venus and suggest a hypothesis of magmatic resurfacing of Venus.

In addition, we perform a direct test of the Frank–Kamenetskii approximation which is used in most studies of temperature-dependent viscosity convection and also provide additional constraints on the transition to stagnant lid convection for non-Newtonian viscosity.

## RHEOLOGY

Any creep mechanism can approximately be described with the help of the following function of temperature  $T$ , shear stress  $\tau$  (second invariant of the deviatoric stress tensor), and hydrostatic pressure  $P$  (e.g., Karato and Wu 1993, Karato and Rubie 1997),

$$\eta = \frac{A}{\tau^{n-1}} \exp \frac{E + PV}{RT}, \quad (1)$$

where  $A$  can approximately be considered a constant,  $R$  is the gas constant,  $E$  is the activation energy,  $V$  is the activation volume and  $n$  is the power-law exponent ( $n \approx 1$  for diffusion creep and  $n \approx 3$ – $3.5$  for dislocation creep).

The largest uncertainty in the question of which creep mechanism dominates in planetary interiors, diffusion creep (Newtonian viscosity), or dislocation creep (non-Newtonian) is the grain size. In the upper mantle of the Earth, grain boundary migration and grain growth seem to be fast enough to produce large grains and make diffusion creep less efficient than dislocation creep (Karato and Wu 1993, Karato 1989). This should be applicable to Venus as well, especially if it is hotter than the

Earth. The lower mantle of Earth was suggested to be in the diffusion creep regime as indicated by the absence of anisotropy (Karato *et al.* 1995, Li *et al.* 1996). However, stagnant lid convection is not very sensitive to the viscosity of the deep interior and is mostly sensitive to the viscosity at the bottom of lithosphere (see below).

It is also worth noting that diffusion creep does not mean Newtonian viscosity because of spatial and temporal variations in grain size (diffusion creep is grain-size dependent!). This implies coupling between kinetics and rheology which results in a strong nonlinear behavior (Solomatov 1996).

The amount of water is also important for the rheology. The question of “wet” versus “dry” mantle is uncertain. It depends on whether or not the interior has efficiently degassed. It has been pointed out that volcanic activity on Venus would result in extensive devolatilization of near surface rocks (Kaula 1990a), implying that “dry” rheologies would be appropriate for the crust and uppermost mantle (Kaula 1995, Mackwell *et al.* 1998). This conclusion is also supported by the observation of slow viscous relaxation of impact craters (Grimm and Solomon 1988).

## SUMMARY OF PREVIOUSLY SUGGESTED SCALING RELATIONSHIPS FOR NON-NEWTONIAN VISCOSITY CONVECTION

### *Nondimensional Parameters*

The viscosity law used in most convection calculations assumes an exponential temperature dependence (Frank–Kamenetskii approximation, see Appendix A),

$$\eta = b\tau^{1-n} \exp(-\gamma T), \quad (2)$$

where  $T$  is the temperature, and  $b$  and  $\gamma$  are constants which depend on the temperature of the isothermal core. The constant  $\gamma = Q/RT_i^2$ , where  $Q$  is the activation enthalpy, and  $T_i$  is the interior temperature.

When the temperature difference between the top and bottom boundaries is fixed, the problem involves two nondimensional parameters: the log viscosity contrast due to temperature alone,

$$\theta = \ln(\Delta\eta) = \gamma \Delta T, \quad (3)$$

which is known as the Frank–Kamenetskii parameter and the Rayleigh number based on the interior temperature,

$$\text{Ra}_i = \frac{\alpha \rho g \Delta T d^{(n+2)/n}}{b^{1/n} \kappa^{1/n} \exp(-\gamma T_i/n)}, \quad (4)$$

where  $\rho$  is the density,  $g$  is the gravitational acceleration,  $\alpha$  is the thermal expansion,  $\Delta T$  is the temperature drop across the layer,  $d$  is the cell size,  $\kappa = k/\rho c_p$  is the thermal diffusivity,  $k$  is the thermal conductivity, and  $c_p$  is the thermal heat capacity at constant pressure.

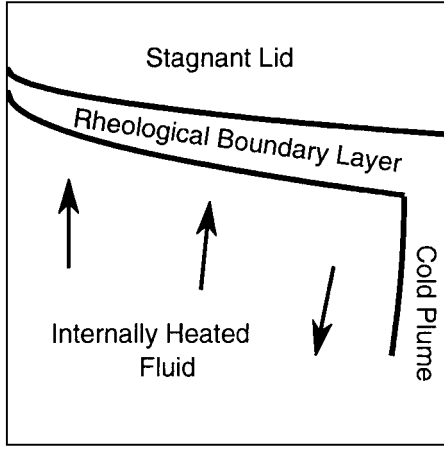


**FIG. 1.** A schematic representation of the stagnant lid convective regime for internal heating. The upper boundary layer is stagnant and only the hottest part of the bottom of the lid actively participates in convection.

### Scaling Theory

The basic features of non-Newtonian stagnant lid convection are similar to those of Newtonian stagnant lid convection (Solomatov 1995). A linear temperature distribution in the lid results in an exponential growth of the viscosity when approaching the surface (Fig. 1). As a result, convection penetrates into the cold lid only by a small length determined by

$$\delta_{\text{rh}} \sim \delta_0 \theta^{-1}, \quad (5)$$

where  $\delta_0$  is the thickness of the stagnant lid. The temperature drop across this thin rheological sublayer is all that is available to drive convection in the interior

$$\Delta T_{\text{rh}} \sim \Delta T \theta^{-1}. \quad (6)$$

Convection beneath the lid is essentially similar to convection with a viscosity depends only on the shear stress driven by the temperature difference scale (6). This gives (see also Appendix B)

$$\text{Nu} \sim \theta^{-\frac{2(n+1)}{n+2}} \text{Ra}_i^{\frac{n}{n+2}} = \theta^{-1.6} \text{Ra}_i^{0.6}, \quad (7)$$

where  $\text{Nu} = Fd/k\Delta T$ . The last equality follows from  $n = 3$ , which is assumed in the numerical calculations discussed below.

### Stability Analysis

Scaling laws can also be obtained using the boundary layer stability argument. As in the case of constant viscosity convection (e.g., Busse 1979), it postulates that the thermal boundary layer is approximately at the margin of convective stability; i.e.,

$$\frac{\alpha \rho g \Delta T \delta_0^{(n+2)/n}}{\kappa^{1/n} b^{1/n} \exp(-\theta/n)} = \text{Ra}_{\text{cr}}, \quad (8)$$

where

$$\text{Ra}_{\text{cr}} = 1568^{1/n} 20^{(n-1)/n} \left[ \frac{e\theta}{4(n+1)} \right]^{2(n+1)/n} \quad (9)$$

is the critical Rayleigh number (Solomatov 1995). This gives the Nusselt number  $\text{Nu} = 1/\delta_0$ ,

$$\begin{aligned} \text{Nu} &\approx \left[ \frac{4(n+1)}{e} \right]^{2(n+1)/(n+2)} 1568^{-1/(n+2)} 20^{-(n-1)/(n+2)} \theta^{-\frac{2(n+1)}{n+2}} \\ &\times \text{Ra}_i^{\frac{n}{n+2}} = 1.18 \theta^{-1.6} \text{Ra}_i^{0.6}. \end{aligned} \quad (10)$$

### Boundary Layer Analysis

An asymptotic boundary layer analysis is possible for a simple model: steady-state, two-dimensional convection with a fixed temperature contrast across the layer and free slip boundary conditions (Morris and Canright 1984, Fowler 1985). For non-Newtonian viscosity, boundary layer solutions were obtained for two end-member models with aspect ratio one (Reese *et al.* 1998). With the assumption that the bottom of the lid is flat,

$$\begin{aligned} \text{Nu} &\approx (1.73)^{3(n+1)/(2n+3)} \theta^{-3(n+1)/(2n+3)} \text{Ra}_i^{n/(2n+3)} \\ &= 2.08 \theta^{-4/3} \text{Ra}_i^{1/3}, \end{aligned} \quad (11)$$

while for variations in lid thickness that scale with the thickness of the lid itself,

$$\text{Nu} \approx (0.88 + 1.15n) \theta^{-1} \text{Ra}_i^{n/(2n+3)} = 4.29 \theta^{-1} \text{Ra}_i^{1/3}. \quad (12)$$

### Numerical Simulations in a $1 \times 1$ Box with Bottom Heating

Numerical simulations in a  $1 \times 1$  box heated from below (Reese *et al.* 1998) gave

$$\text{Nu} \approx 2.8 \theta^{-0.96} \text{Ra}_i^{0.29}. \quad (13)$$

Although this relationship is in approximate agreement with boundary layer theory, we observed that the aspect ratio of the convective cells started to vary at high Rayleigh numbers even in this  $1 \times 1$  box. Since the results strongly depend on the aspect ratio (Morris and Canright 1984, Fowler 1985, Tackley 1993), the above relationship might cause substantial errors when extrapolating to high  $\text{Ra}_i$  and  $\theta$ .

## TRANSITION TO STAGNANT LID CONVECTION

Several runs in a  $1 \times 1$  convective box with bottom heating (Fig. 2) confirmed the prediction that the transition to stagnant lid convection does not depend much on the Rayleigh number and occurs at a viscosity contrast across the cold boundary layer of around  $e^{4(n+1)}$  (Solomatov 1995, Solomatov and Moresi 1997). For  $\exp(\theta) = 10^8$ , which is close to the transition, low resolution cases showed intermittent behavior with the solution oscillating between the regimes. Higher resolution runs eliminated this intermittent behavior and gave stagnant lid convection.

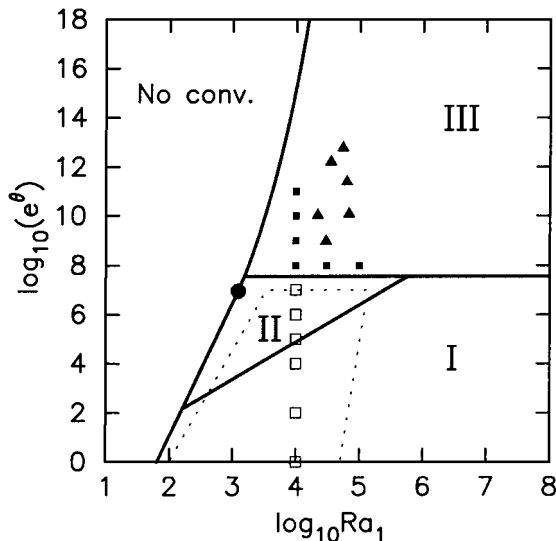


**FIG. 2.** The parameter range explored in this and previous works is shown on the regime diagram estimated for non-Newtonian viscosity convection (Solomatov 1995): Christensen's (1985a) data are located within the dashed contour. The  $1 \times 1$  convection experiments from Solomatov and Moresi (1996) and Reese *et al.* (1998) with two extra points for  $\exp(\theta) = 10^8$  and  $Ra_1 = 3 \times 10^4$  and  $10^5$  are indicated with solid and open boxes where solid boxes indicate stagnant lid regime. The  $4 \times 1$  convection experiments with internal heating are indicated with triangles. Note that the location of the experiments with internal heating is only tentative since this is a somewhat different problem (no bottom boundary layer across which the viscosity contrast is around 10). The convective regimes indicated are: I, the small viscosity contrast regime; II, the transitional regime; and III, the stagnant lid regime.

### NUMERICAL SIMULATIONS IN A $4 \times 1$ BOX WITH INTERNAL HEATING

In this section we consider a large aspect ratio box ( $4 \times 1$ ) in which the cell size is established naturally. We also consider internally heated convection which is more appropriate for mantle dynamics. Six such cases were run on a  $128 \times 32$  mesh:  $(Ra_{H,0}, \theta) = (10, 60), (30, 60), (3, 70), (3, 80), (10, 80), (30, 80)$ . The Rayleigh number  $Ra_{H,0}$  is based on the internal heating rate  $H$ ,

$$Ra_{H,0} = \frac{\alpha \rho^2 g H d^{(3n+2)/n}}{k b^{1/n} \kappa^{1/n}}. \quad (14)$$

Note that since the nondimensional temperature at the bottom is not unity as in the previous problem but  $T_1 = T_i = Nu^{-1}$  (for internally heated convection it is convenient to define the interior temperature  $T_i$  as the bottom temperature  $T_1$ ), the actual viscosity contrast between the top and the bottom due to temperature alone is

$$\Delta \eta = \exp(\gamma T_i) = \exp(\theta/Nu). \quad (15)$$

In the simulations, the viscosity contrast is between  $10^9$  and  $10^{13}$  which is large enough for the stagnant lid to form (Fig. 2).

The measurements were taken as follows. After a thermal equilibrium between the internal heat production rate and the cooling rate is reached with approximately 1% accuracy, the runs were continued for a sufficiently long time period so that the Nusselt number error due to fluctuations dropped below 1%.

One test performed on a  $256 \times 64$  mesh showed that errors due to resolution (Fig. 3) are comparable with errors due to fluctuations. As a result, a 1–2% error is estimated for the Nusselt number and about 3% for the rms bottom velocity. Additional resolution tests can be found in Solomatov and Moresi (1997).

The asymptotic scaling formula for the  $Nu$ – $Ra$  relationship (Fig. 4) is (Appendix B)

$$Nu \approx 0.98 \theta^{-1.6} Ra_i^{0.6}. \quad (16)$$

The above equation differs from scaling laws obtained theoretically and numerically for a  $1 \times 1$  box (Eqs. (11), (12), (13)). On the other hand, it agrees well with scaling theory and stability analysis (Eqs. (7), (10)). It is also consistent with the scaling for Newtonian viscosity suggested by laboratory experiments (Davaille and Japaurt 1993) and numerical simulations in a  $2 \times 1$  box (Grasset and Parmentier 1998). The discrepancy is due to the fact that in a  $1 \times 1$  box, the aspect ratio of the convective cell is fixed while in long boxes the effect of walls is small and the aspect ratio of the convective cells can vary naturally; i.e., it changes in such a way as to keep the thickness of the stagnant lid near critical (Eq. (10)).

The asymptotic scaling formula for the rms velocity in the actively convecting part of the layer is (Appendix B)

$$u \approx 0.05 \left( \frac{\kappa}{d} \right) \theta^{-1.2} Ra_i^{1.2}. \quad (17)$$

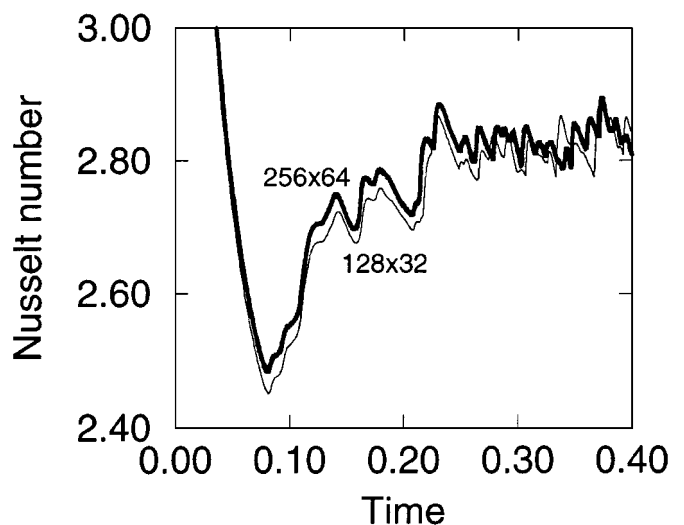


**FIG. 3.** A resolution test for internally heated convection in a  $4 \times 1$  box. The beginning of the curves  $Nu(t)$  for  $128 \times 32$  and  $256 \times 64$  meshes are shown. The asymptotic time-averaged values of the Nusselt number and the velocity are  $Nu = 2.90 \pm 0.02$ ,  $u = 75 \pm 2$  for the  $128 \times 32$  mesh and  $Nu = 2.93 \pm 0.02$ ,  $u = 73 \pm 2$  for the  $256 \times 64$  mesh.

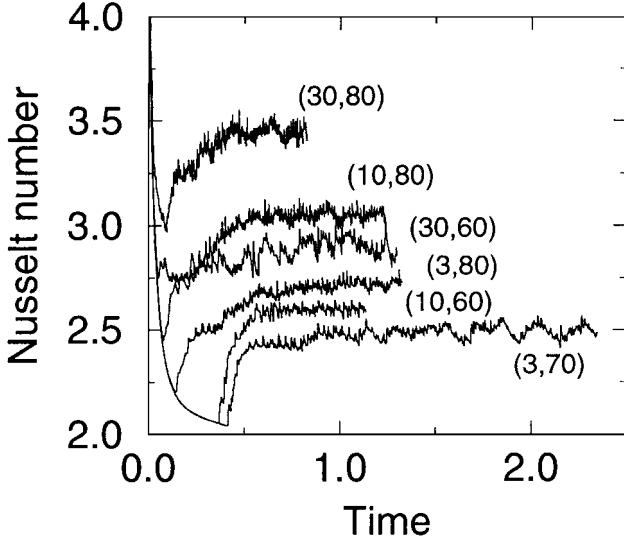


**FIG. 4.** Nusselt number as a function of time for internally heated convection in a  $4 \times 1$  box. The labels indicate the values of the Rayleigh number  $Ra_{H,0}$  and the Frank–Kamenetskii parameter  $\theta$ :  $(Ra_{H,0}, \theta) = (10, 60), (30, 60), (10, 70), (3, 80), (10, 80), (30, 80)$ .

#### Pressure-Dependent Viscosity

The effect of pressure has important consequences for the properties of convection (see, e.g., Christensen 1985b, van den Berg and Yuen 1997, Doin *et al.* 1997). Here we test the hypothesis that the lid thickness is controlled by the total viscosity gradient in the lid, due to both temperature and pressure (Doin *et al.* 1997). We consider pressure-dependent viscosity in the form (e.g., Christensen 1985a)

$$\eta = c\tau^{1-n} \exp(-\theta_T T + \theta_z z) \quad (18)$$

where  $c$ ,  $\theta_T$ , and  $\theta_z$  are constants.

The stability conditions in the rheological sublayer at the bottom of the lid and the lid thickness would be the same for both (18) and (2) if the viscosities and viscosity gradients at the bottom of the thermal boundary layer are the same; i.e.,

$$\exp(-\theta T) = c \exp(-\theta_T T + \theta_z z), \quad (19)$$

$$\theta = \theta_T - \theta_z \frac{dz}{dT}, \quad (20)$$

**TABLE I**  
**Pressure-Dependent Viscosity**

$Ra_{H,0}$	$\theta$	$\theta_T$	$\theta_z$	$c$	Nu	$u_{rms}$
10	80	80	0	1	3.05	115
10	80	88.52	5	2.07	3.04	76
10	80	97.04	10	4.29	3.01	61
30	80	80	0	1	3.45	131
30	80	87.71	5	1.61	3.44	95
30	80	95.43	10	2.60	3.40	77

where the parabolic temperature profile in the lid suggests (see Appendix B)

$$\frac{dz}{dT} = (1 - 2Nu^{-1})^{-1/2}. \quad (21)$$

This gives the following formulae for  $\theta_T$  and  $c$ :

$$\theta_T = \theta + \theta_z(1 - 2Nu^{-1})^{-1/2} \quad (22)$$

$$c = \exp\left[\frac{\theta - \theta_T}{Nu} - \theta_z\left(1 - \left(1 - \frac{2}{Nu}\right)\right)^{1/2}\right]. \quad (23)$$

Numerical tests show that the Nusselt number obtained this way is, indeed, almost independent of  $\theta_z$  despite pressure-induced viscosity variations of up to  $\exp(\theta_z) = 2.2 \times 10^4$  (Table I).

### PARAMETERIZATION OF CONVECTION WITH ARRHENIUS TEMPERATURE AND PRESSURE DEPENDENT NON-NEWTONIAN VISCOSITY

#### Nusselt Number

Summarizing the results from (Davaille and Japaurt 1993, Solomatov 1995, Doin *et al.* 1997; Grasset and Parmentier 1998) for Newtonian viscosity and the results of this study for non-Newtonian viscosity, the following asymptotic scaling can be suggested for the original Arrhenius viscosity (1):

$$Nu \approx [0.47 + 0.25(n-1)]\theta^{-\frac{2(n+1)}{n+2}} Ra_i^{\frac{n}{n+2}}. \quad (24)$$

The generalized Frank–Kamenetskii parameter is

$$\theta = \left| \Delta T \frac{d \ln \eta}{dT} \right| = \frac{\Delta T (E + P_i V)}{RT_i^2} - \frac{P_i V}{RT_i}, \quad (25)$$

where  $P_i$  is calculated at the bottom of the thermal boundary layer. The generalized Rayleigh number is

$$Ra_i = \frac{\alpha \rho g \Delta T d^{(n+2)/n}}{b^{1/n} \kappa^{1/n} \exp[(E + P_i V)/n RT_i]}. \quad (26)$$

The error in the prefactor in (24) is perhaps around 30% due to experimental error, a limited number of values of  $n$  studied ( $n = 1$  and  $3$ ), inaccuracy of the Frank–Kamenetskii approximation (see Appendix A), and 2-D geometry of numerical experiments.

#### Velocity

For the velocity scale we will use the following formula (17)

$$u \approx 0.05 \zeta \frac{\kappa}{d} \theta^{-2n/(n+2)} Ra_i^{2n/(n+2)}, \quad (27)$$

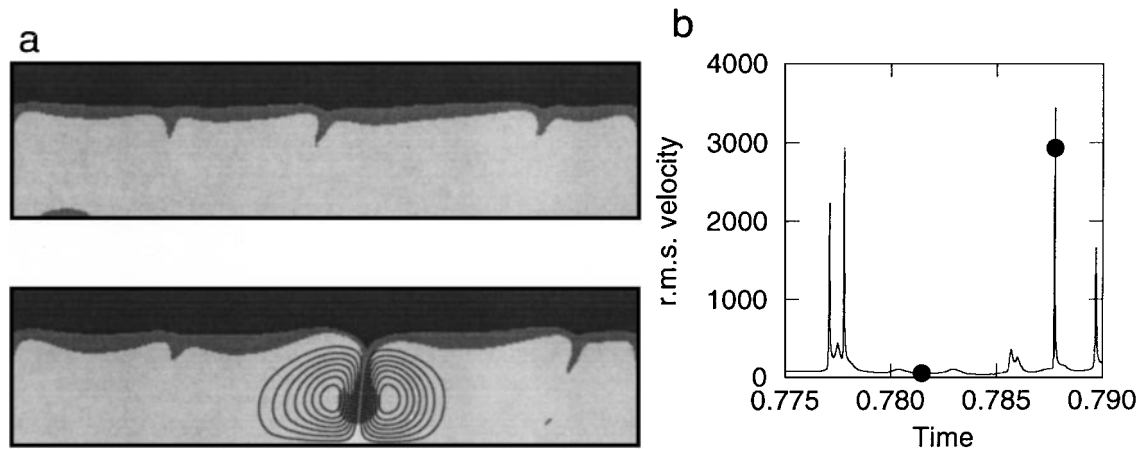


**FIG. 5.** (a) Two snapshots of internally heated non-Newtonian viscosity convection for  $Ra_{H,0} = 30$ ,  $\theta = 80$ . (Top) Slow convection period. (Bottom) Avalanche-like instability developed at the bottom of the cold thermal boundary layer. Note that the instability involves only a small fraction of the boundary layer. The coldest part of it is stagnant (the darkest layer) and does not participate in convection in the interior. (b) Location of the snapshots on the rms velocity versus time curve (black dots).

where  $\zeta$  is a correction factor needed to take into account pressure-dependent viscosity and phase boundaries. Our calculations suggest that the rms velocity does not drop by more than a factor of 2 even for pressure-induced viscosity variations of around  $10^3$  in the actively convecting part of the layer (Table I), which is similar to the expected viscosity variation in Earth (e.g., King 1995). The spinel–perovskite transition around 700 km could also be a partial barrier for convection and can somewhat decrease  $\zeta$  (velocity scales approximately linearly with the size of the convective cells). We will use  $\zeta \approx 0.4$ . The dependence of the prefactor on  $n$  is assumed to be weak.

## THERMAL EVOLUTION MODELS

### *Global Resurfacing on Venus*

Global resurfacing on Venus around 300–800 Myr ago is an important constraint on the thermal evolution of Venus (Schaber *et al.* 1992, Phillips *et al.* 1992, Bullock *et al.* 1993, Namiki and Solomon 1994, Herrick and Phillips 1994, Price *et al.* 1996, Hansen and Willis 1996, Grosfils and Head 1996, Basilevsky *et al.* 1997, McKinnon *et al.* 1997). Previous models of global resurfacing include widespread melting caused by phase transformation-induced transition from layered to whole mantle convection (Steinbach and Yuen 1992), periodic instabilities of a depleted layer beneath the crust (Parmentier and Hess 1992, Herrick and Parmentier 1994), transition from oscillatory to quasi-steady state circulation (Arkani-Hamed *et al.* 1993), some kind of episodic plate tectonics (Turcotte 1993, Weinstein 1996, Fowler 1996, Moresi and Solomatov 1998), and cessation of plate tectonics (Herrick 1994, Solomatov and Moresi 1996). The global resurfacing model suggested below is due to magmatism alone. It is assumed that Venus remains in the stagnant lid regime during its entire evolution.

### *Conductive Regime*

For any rheological law, an isothermal or adiabatic mantle can initially be stable even at temperatures near the solidus. In this case, the planet removes internally generated heat by conduction.

An example of the conductive history of Venus with an initial mantle temperature  $T_0 = 1400$  K and a specific heat generation rate  $H(t) = H_0 \exp[-\lambda(t - t_0)]$  (Carslaw and Jaeger 1959) is shown in Fig. 6 along with the melting curve (Fig. 7).

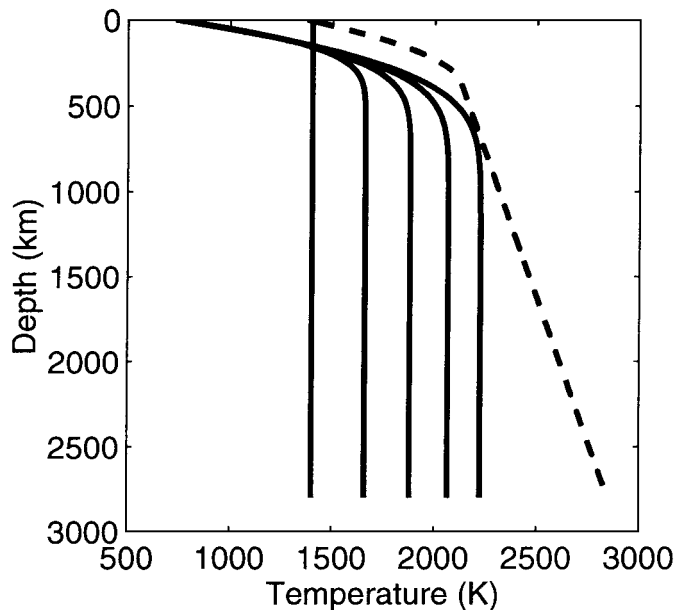


**FIG. 6.** An example of the evolution of the temperature profile in the conductive regime. The initial temperature is 1400 K and the surface temperature is 730 K. The profiles are plotted every 0.5 Gyr. Melting is suppressed until  $\sim 2$  Gyr due to the formation of a thick cold thermal boundary layer.

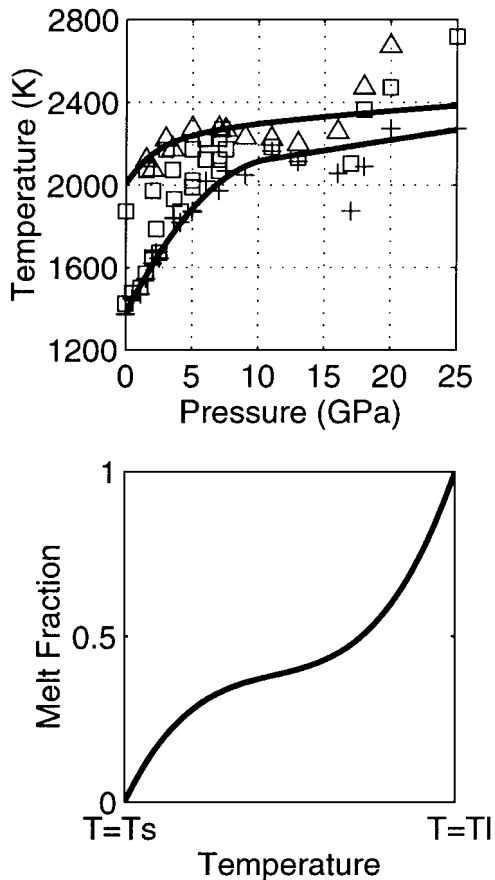


**FIG. 7.** Solidus, liquidus, and partial melt experimental data for peridotite from McKenzie and Bickle (1988), Scarfe and Takahashi, (1986), and Ito and Takahashi (1987). The liquid region is marked with triangles, the solid region with crosses, and the partially molten region with squares. The solidus of the mantle is parameterized as  $T = 1374 + 130P - 5.6P^2$ , where the temperature is in Kelvin and the pressure in gigapascals. After the slope reaches  $dT/dP = 10 \text{ K GPa}^{-1}$ , the temperature increases linearly with pressure. The liquidus and melt fractions are given by the expressions of McKenzie and Bickle (1988).

Parameter values for Venus are given in Table II. The internal heat production rate is assumed to be similar to the terrestrial one:  $H_0 = 4.8 \times 10^{-12} \text{ W/kg}$ ,  $\lambda = 0.3328 \text{ Gyr}^{-1}$ , and  $t_0 = 4.5 \text{ Gyr}$  (Namiki and Solomon 1998). The temperature profile is plotted at intervals of 0.5 Gyr. Although pressure effects and other factors are not taken into account, it is clear that, in the absence of convection, significant melting would not occur until  $\sim 2 \text{ Gyr}$  due to the development of a thick cold thermal boundary layer at the surface. For this part of planetary evolution, the heat flux, after a rapid initial drop, remains essentially constant.

#### Parameterized Convection

As the interior temperature increases, convective instabilities develop near the bottom of the lithosphere. This is the stagnant lid regime. The time until the onset of convection depends on the initial potential temperature, heating rate, and viscosity model.

**TABLE II**  
Definitions and Values of Parameters

Parameter	Notation	Value
Depth of convective layer	$d$	2900 km
Thermal conductivity	$k$	3.2 W/m K
Thermal expansion	$\alpha$	$3 \times 10^{-5} \text{ K}^{-1}$
Density	$\rho$	$3300 \text{ kg m}^{-3}$
Acceleration due to gravity	$g$	$8.9 \text{ m s}^{-2}$
Thermal diffusivity	$\kappa$	$8 \times 10^{-7} \text{ m}^2 \text{ s}^{-1}$
Surface temperature	$T_s$	730 K

Two parameterizations are considered. The first is similar to that used by Schubert *et al.* (1997) and Grasset and Parmentier (1998) for Newtonian viscosity. The activation enthalpy is assumed to be constant during evolution and is calculated at some effective depth. The second is based on Eqs. (24)–(27). Figure 8 and Table III show results for two models, (a) and (b), corresponding to these two parameterizations, respectively.

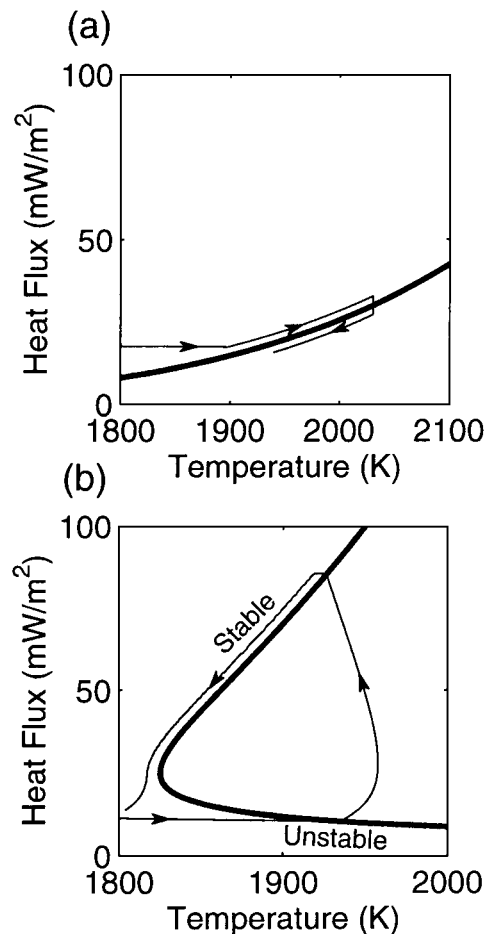


**FIG. 8.** Stability curves and thermal evolution for (a) constant and (b) pressure-dependent activation enthalpy (Table III). For pressure-dependent viscosity, the upper and lower branches correspond to stable and unstable equilibrium lid thicknesses, respectively. The onset of convection occurs on the lower branch followed by relaxation to the stable branch.

**TABLE III**  
**Model Results**

Parameter	Model (a) <sup>a</sup>	Model (b)
Initial temperature (K)	1200	1400
Heating rate <sup>b</sup>	1	0.5
Activation energy (kJ)	430	540
Activation volume ( $10^{-5}$ m <sup>3</sup> /mol)	1.5	2.5
Power law exponent $n$	3.0	3.5
Preexponential factor ( $10^{15}$ GPa <sup><math>n</math></sup> s)	.26	4.1
Mantle heat flux (mW/m <sup>2</sup> )	18	14
Lid thickness (km)	200	250
Crustal thickness (km)	45	70

<sup>a</sup> Enthalpy is constant during evolution and is calculated at  $P = 12.8$  GPa.

<sup>b</sup> Relative to chondritic value corresponding to present-day heat production of  $4.8 \times 10^{-12}$  W/kg.

The dependence of heat flux on temperature (which is also approximately the stability curve for initiation of convection) is very different for these two models (Fig. 8). Model (a) is characterized by a monotonic increase of the heat flux with temperature. In Model (b), there are two branches corresponding to stable (upper branch) and unstable (lower branch) equilibrium lid thicknesses (Doin *et al.* 1997). Convection starts on the lower branch and is followed by thermal relaxation of the lid to the upper branch.

The thermal evolution for pressure-dependent viscosity is calculated as follows. To take into account thermal relaxation during thinning of the lid, energy balance equations for both the lid and the mantle are considered,

$$M_m c_p \frac{\partial T_i}{\partial t} = M_m H_m(t) - F S_m \quad (28)$$

$$M_{\text{lid}} c_p \frac{\partial \bar{T}}{\partial t} = M_{\text{lid}} H_{\text{lid}}(t) - F_0 S_0 + F S_m, \quad (29)$$

where  $M_m$  and  $M_{\text{lid}}$  are the mass of the mantle and lid, respectively,  $T_i$  is the mantle temperature,  $\bar{T}$  is the volume averaged lid temperature,  $H_m$  and  $H_{\text{lid}}$  are the heat generation rate in the mantle and lid, respectively,  $S_0$  is the surface area of Venus,  $S_m$  is the surface area at the upper boundary of the mantle,  $F = k(T - T_s)/d$  Nu, where  $T_s$  is the surface temperature, and  $F_0$  is the heat flux at the onset of convection. The temperature distribution in the lid during lid thinning is modeled as two linear segments. The heat flux at surface of the lid is equal to the convective heat flux at the onset of convection. The heat flux at the bottom of the lid matches the convective heat flux during relaxation. Note that in writing (28) and (29), terms corresponding to changes in energy due to the moving boundary are neglected. This assumption is valid if the lid relaxation is slow enough so that the rate of change of the lid energy due to the moving boundary is small with respect to the net rate of change of the energy associated with heating/cooling. After the lid thickness reaches the stable equilibrium, a one-layer model (28) is used to

calculate the thermal evolution. Equation (28) is also used for the constant activation enthalpy model.

### Melting

After convection starts, upwelling flow begins to melt at the depth where the mantle temperature intersects the solidus curve. The liquidus temperature and melt fraction are given by the expressions of McKenzie and Bickle (1988). To determine the melting rate, notice that for a simple uniform flow beneath the stagnant lid, the depth range between the beginning of melting and the bottom of the stagnant lid,  $z_m$ , determines the width of the horizontal flow which underwent melting (Fig. 9). The rate at which material passes through this channel is simply  $u_i z_m 2\pi d$ , where  $u_i$  is the average interior velocity (see Eq. (27)). The rate of melt production is  $u_i z_m 2\pi d \Phi$ , where  $\Phi$  is the volume fraction of the layer which is molten. If all of the melt is transported to the surface the corresponding volcanic flux is given by

$$F_{\text{vol}} \sim 2u_i z_m \Phi / d. \quad (30)$$

### Differentiation

Decompression melting of upwelling material in the mantle produces buoyant magmas which extract heat-producing elements and are deposited on or near the surface. For a planet with plate tectonics, subduction of the lithosphere can effectively remix radioactive elements with the mantle. However, when planetary lithospheres stagnate uppermost material is not easily advected downward and remixing of heat sources is more difficult. An end-member model of irreversible fractionation is considered in which all heat producing elements of the upper mantle are extracted upon partial melting. For very incompatible elements such as U, Th, and K, this is a reasonable assumption (Anderson 1989). Differentiation reduces the internal heat production rate and lowers mantle temperatures, preventing further

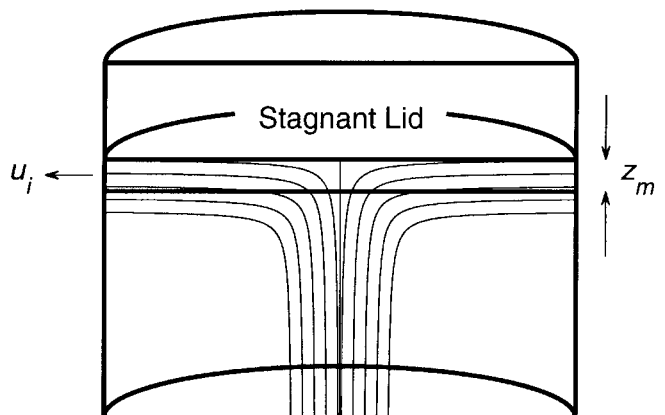


**FIG. 9.** Schematic illustration of the mantle differentiation model. Partial melting begins at a depth  $z_m$  beneath the lid where the temperature intersects solidus. The characteristic time for depletion is  $(z_m/d)u/d$ , where  $d$  is the depth of the layer.

melting and differentiation (Schubert *et al.* 1992, Kaula 1994, Turcotte 1996, Schubert *et al.* 1997).

The differentiation rate is estimated as follows. If, before melting, the concentration of radioactive elements is  $C$ , the chemical flux through the partially molten region is  $u_1 C z_m 2\pi d$ . Since all radioactive elements are assumed to be nearly completely extracted from the rocks, this gives an estimate for the chemical loss rate from the mantle. The rate of decrease of the total amount of radioactive elements in the cell is  $d(C\pi d^3)/dt$ . Therefore,

$$\frac{dC}{dt} \approx -2C \frac{z_m}{d} \frac{u}{d}, \quad (31)$$

where the interior velocity is parameterized with the help of (27).

## RESULTS

After the initial conductive evolution, where melting is suppressed due to the thick thermal boundary layer, convection begins. The mantle heat flux increases rapidly and quickly exceeds the critical heat flux for melting. As a result of differentiation associated with magmatism, the residual mantle heat production rate drops below the heat loss rate (which depends on the temperature and therefore cannot respond immediately to the reduced heating rate), the planet cools, the lid thickens, and melting ceases. Note that in contrast to previous models of planetary evolution the present-day state depends on the initial conditions.

The parameters which are varied are viscosity (“wet” versus “dry” and activation volume), the initial temperature, and heating rate. The initial potential temperature, however, cannot be far from the solidus temperature at the surface—the melting curve is convectively unstable and would tend to drop to an adiabat starting at the surface solidus temperature or slightly higher (Solomatov and Stevenson 1993). The initial mantle heating rate may vary due to compositional heterogeneity of accreting material (O’Nions *et al.* 1979) and/or differentiation associated with the formation of stable primary crust (Taylor 1989). The point is that different combinations of the parameters can give the same results: cessation of extensive melting on Venus 300–800 Myr ago.

Since the mechanisms of magma transport and crustal recycling in the stagnant lid regime are poorly understood, volcanic rates have simply been scaled according to estimates of crustal production on Venus (Grimm and Hess 1997, Price and Suppe 1994, Namiki and Solomon 1994, Head *et al.* 1991).

In Fig. 10, Model (a) predicts a volcanic flux at the end of resurfacing 300–800 Myr ago of about  $2 \text{ km}^3/\text{year}$ , which is sufficient to resurface kilometer-high topography in about 250 Myr. The magmatic period lasts for about 2.5 Gyr. Model (b) predicts onset of convection at 1.5 Gyr ago and an avalanche-like episode of melting and differentiation which lasts for only  $\sim 1$  Gyr. Lithospheric thickening due to cessation of convection  $\sim 0.2$  Gyr ago suppresses present day volcanism on Venus.

## DISCUSSION AND CONCLUSIONS

1. The transition to stagnant lid convection for dislocation creep occurs at a viscosity contrast due to temperature alone of  $10^7$ – $10^8$ . This is higher than the value of  $10^4$ – $10^5$  for Newtonian viscosity convection, yet much smaller than the viscosity contrasts expected for the terrestrial planets. With typical values of the activation enthalpy for dislocation creep (Karato and Wu 1993), and near solidus temperatures of planetary interiors, a stagnant lid would form at surface temperatures around 1000–1100 K, while the surface temperature on Venus is only 730 K. In the absence of brittle fracture, stagnant lid convection seems the most likely convective style of Venus.

2. Compared to stagnant lid convection with Newtonian viscosity, the flow is concentrated in a few places while the rest of the mantle is quiescent. The flow is highly time-dependent with periods characterized by avalanche-like instabilities at the bottom of the lid, followed by relatively quiet periods of slow convective motion. This seems to be a typical feature of non-Newtonian viscosity convection (Larsen *et al.* 1996, Larsen and Yuen 1997, Larsen *et al.* 1997). Also, lateral variation in lid thickness is observed to be much smaller than for Newtonian viscosity. This should affect gravity and topography signals, stress distribution in the lid, and initiation of plate tectonics (Fowler 1993; Fowler and O’Brien 1996).

3. Although the results of numerical simulations of bottom heated convection in a  $1 \times 1$  box are in reasonable agreement with boundary layer analysis, such small domain calculations do not allow the aspect ratio of the convection cells to develop naturally. This problem was eliminated by performing numerical simulations of internally heated convection in a  $4 \times 1$  box. The scaling relationships are in good agreement with scaling theory and boundary layer stability analysis. Scaling relationships for the general temperature- and pressure-dependent Arrhenius viscosity law (1) are summarized by Eqs. (24)–(27). Stagnant lid convection is sensitive to the viscosity and total viscosity gradient at the bottom of the lid.

4. Initial potential temperature near solidus could be insufficient to initiate convection, implying that the planet evolves in the conductive regime. Melting and differentiation are suppressed until a later time in evolution. Initiation of stagnant lid convection results in lithospheric thinning and widespread melting and volcanism. The end of extensive volcanism corresponds to the age of resurfacing around 300–800 Myr ago. The thickness of the present-day venusian lithosphere turns out to be around 200 km which is intermediate compared to previously suggested estimates (McKenzie 1994, Kucinskas and Turcotte 1994, Phillips 1994, Smrekar 1994, Smrekar and Parmentier 1996, Solomatov and Moresi 1996, Moore and Schubert 1997, Nimmo and McKenzie 1997, Nimmo and McKenzie 1998, Simons *et al.* 1997, Smrekar *et al.* 1997). The models also suggest that the lithosphere was thinner in the past (especially if magmatism could mobilize the lithosphere as discussed below), which is consistent with geological models (Brown and Grimm

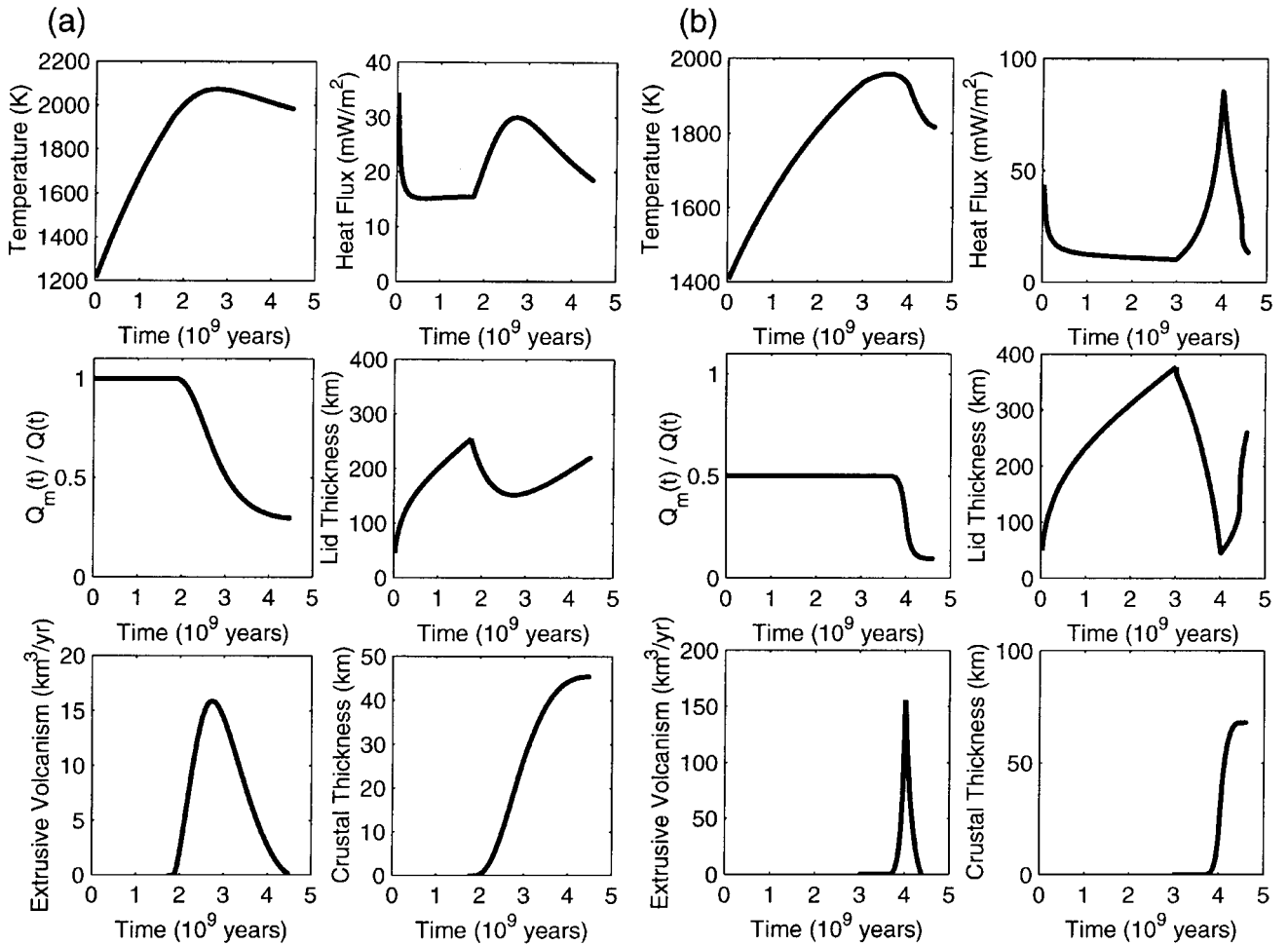


**FIG. 10.** Stagnant lid thermal evolution models for Venus including melting and differentiation. Convection is parameterized using the  $Nu(Ra)$  relations for internal heating in a  $4 \times 1$  box. The model parameters are given in Table III. Note that melting and differentiation are suppressed until later in planetary evolution.

1997, Hansen and Willis 1998, Phillips and Hansen 1998, Head and Basilevsky 1998).

5. Further understanding of the thermal evolution of Venus requires a better description of the effects of melting on mantle convection. In particular, it is conceivable that extensive magmatism could weaken the lithosphere and cause lithospheric recycling. This would be further enhanced if the surface temperature increased as a result of volcanism-induced changes in atmospheric composition (Bullock and Grinspoon 1996). This would not only affect the surface geology through the generation of thermal stresses (Solomon *et al.* 1998), but also could reduce the viscosity of the upper layers and help to mobilize the lid.

The fraction of melt which can penetrate the cold stagnant lid is unknown (e.g., Watson and McKenzie 1991, Nimmo and McKenzie 1998). Since the lithospheric thickness varies with time, this would affect the evolution of volcanic activity. Additionally, the rheology controlling convection beneath the lid would be affected by melt retained in the mantle (Kohlstedt and Zimmerman 1996). Also, melt buoyancy can lead to Rayleigh–Taylor instabilities (Tackley and Stevenson 1993).

Chemical stratification is another poorly understood consequence of melting. Extraction of melt from the layer beneath the lid might eventually lead to some kind of stable two-layered mantle convection or the formation of a buoyant melt residuum layer that could subsequently become cool and dense enough to detach (Parmentier and Hess 1992, Herrick and Parmentier 1994).

Finally, the gabbro–eclogite phase transformation also plays an important role in planetary thermal evolution by providing a mechanism for the recycling of crustal material (Anderson 1980, Namiki and Solomon 1993).

#### APPENDIX A: THE ACCURACY OF THE FRANK–KAMENETSKII APPROXIMATION

The Frank–Kamenetskii approximation assumes that the Arrhenius viscosity law can be approximated by an exponential law suggesting viscosity contrasts which are many orders of magnitude smaller at the surface. Although there were several discussions of this approximation (e.g., Fowler 1985, Solomatov and Moresi 1996, Ratcliff *et al.* 1997) a direct comparison between exponential and Arrhenius laws is absent.

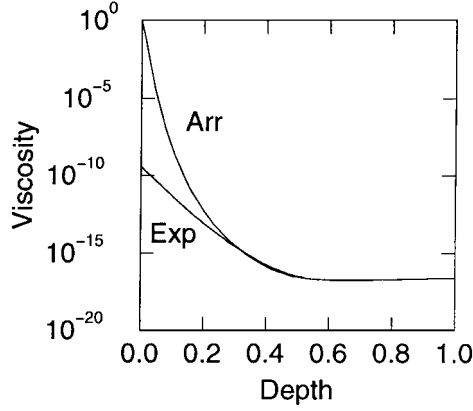


**FIG. 11.** Viscosity as a function of depth for exponential and Arrhenius viscosity laws.

To investigate the accuracy of the Frank–Kamenetskii approximation, we first obtained a steady-state solution ( $32 \times 32$  mesh) for internally heated convection with Newtonian Arrhenius viscosity  $\eta = b \exp[A/(T + T_0)]$ , where  $b = 8.756511 \times 10^{-27}$ ,  $A = 12.0$ ,  $T_0 = 0.2$ , and  $\text{Ra}_0 = 10^{-10}$ . These nondimensional parameters are close to the parameter range for Venus.

The corresponding exponential law is calculated as follows. The theoretical value of the Frank–Kamenetskii parameter is calculated based on the bottom temperature  $T = T_1 = 0.353$  (for an internally heated convection this temperature represents the temperature of the actively convection interior):  $\theta = A/(T_1 + T_0)^2 \approx 39.2$ . The prefactor in the exponential law  $\eta = b \exp(-\theta T)$  with this value of  $\theta$  is chosen in such a way as to get the same bottom Rayleigh number (calculated at the bottom viscosity). Calculations with this Rayleigh number and exponential viscosity showed that the temperature is lower by about 4–5%. This is basically the accuracy of Frank–Kamenetskii approximation in determining the mantle temperature.

Another way to look at this problem is to find iteratively such an exponential law which gives the closest match to the Arrhenius law. The match was achieved at  $\eta = 3.91 \times 10^{-10} \exp(-47T)$  (Figs. 11 and 12). The value of  $\theta \approx 47$  is about 20% higher than the theoretical value of 39.2. Since  $\text{Nu} \propto \theta^{-\beta}$ , where  $\beta$  is around 1, this difference implies that Nu–Ra relationships obtained with an exponential law overestimate the prefactor in Nu–Ra relationship by about 20%.

A somewhat lower heat transport efficiency of the Arrhenius law is due to an increasingly faster growth of the viscosity when moving from the interior to the surface. This makes the unstable sublayer at the bottom of the stagnant lid a little thinner, reducing the driving force for convection.

## APPENDIX B: ASYMPTOTIC SCALING BASED ON LOW NUSSELT NUMBER CALCULATIONS

Although convection in our calculations is extremely vigorous and time-dependent, the lid is too thick and the asymptotic state  $\text{Nu} \ll 1$ ,  $\theta \gg 1$  has not been reached yet. To obtain a correct scaling relationship, we need to take into account the fact that convection occurs only in a portion of the convective layer beneath the stagnant lid (Grasset and Parmentier 1998).

We assume that convection beneath the lid is driven by the rheological temperature scale  $\Delta T_{\text{rh}}$  which is proportional to  $\gamma^{-1}$ :

$$F_{\text{eff}} = a \frac{k\gamma^{-1}}{d_{\text{eff}}} \left( \frac{\alpha \rho g \gamma^{-1} d_{\text{eff}}^{(n+2)/n}}{b^{1/n} \kappa^{1/n} \exp(-\gamma T_1/n)} \right)^\beta, \quad (\text{B1})$$

where  $a$  and  $\beta$  are constants,  $n = 3$ , and

$$d_{\text{eff}} = d - \delta_L \quad (\text{B2})$$

is the thickness of the convecting layer beneath the lid. The effective heat flux which drives convection beneath the lid can also be expressed as

$$F_{\text{eff}} = \rho H d_{\text{eff}}. \quad (\text{B3})$$

The relationship between the lid thickness  $\delta_L$  and the temperature at the bottom of the lid can be found from the steady-state conductive profile in the lid,

$$T_L = \frac{F_{\text{eff}} \delta_L}{k} + \frac{\rho H \delta_L^2}{2k}. \quad (\text{B4})$$

If we assume that the lid is the cold thermal boundary layer, then  $T_L = T_i$ . A somewhat more accurate determination of the lid thickness is obtained if we take into account that the actual lid is thinner than the thermal boundary layer by a small amount determined by the thickness of the rheological boundary layer (5). With this correction,  $T_L = T_i - a_{\text{rh}} \gamma^{-1}$ , where  $a_{\text{rh}}$  is a numerical coefficient. The final formula relating  $\text{Ra}_{H,0}$ ,  $\theta$ , and

$$\text{Nu} = \frac{\rho H d^2}{k T_i} \quad (\text{B5})$$

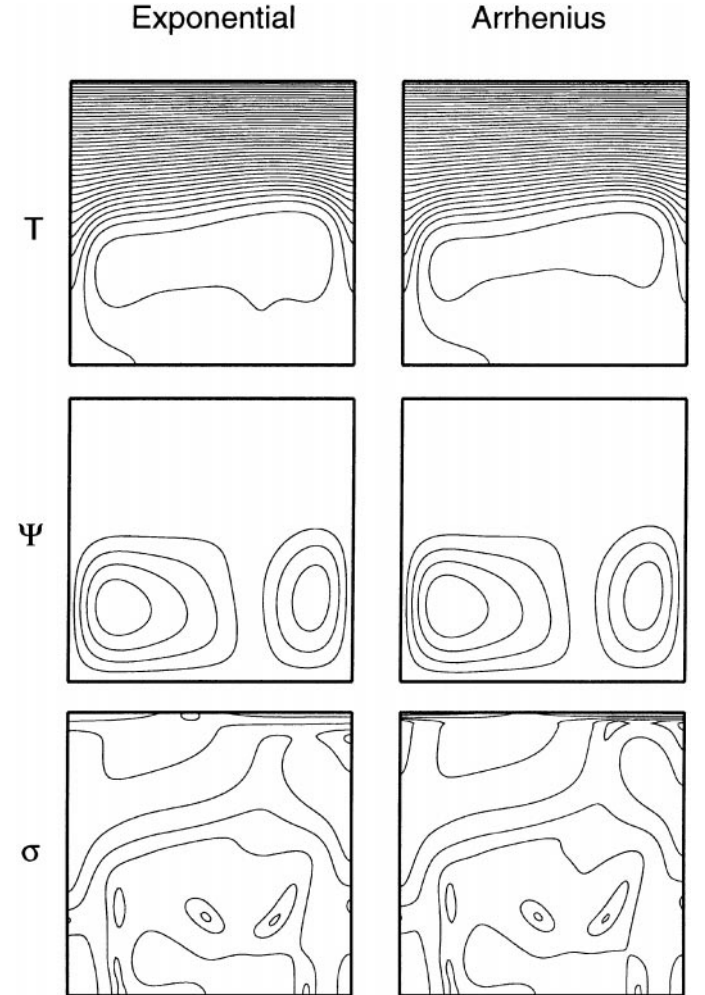


**FIG. 12.** Comparison between exponential and Arrhenius viscosity laws: temperature  $T$ , stream function  $\Psi$ , and the second invariant of the stress tensor  $\sigma$ . Except for the stress boundary layer at the surface, the discrepancies are small despite viscosity differences of 10 orders of magnitude (Fig. 11).

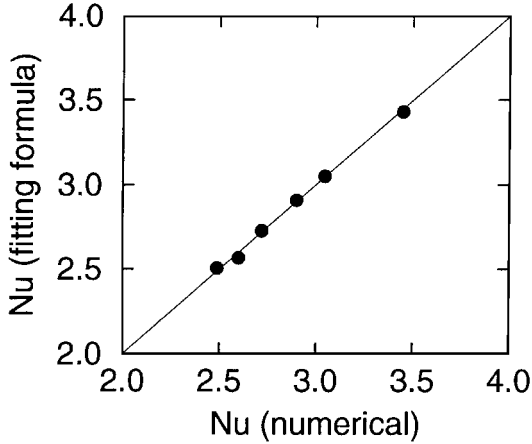


**FIG. 13.** The results of the fit for the Nusselt number: the values calculated using the fitting formula (B6) versus the numerical data.

is

$$(1 - 2Nu^{-1} + 2a_{th}\theta^{-1})^{1-\beta(n+2)/2n} = a\theta^{-(1+\beta)}Ra_{H,0}^{\beta} \exp(\beta\theta/nNu). \quad (B6)$$

A two-parameter fit gives  $\beta = 0.70 \pm 0.06$ . Using the theoretical value  $\beta = n/(n+2) = 0.6$ , we obtain  $a = 0.98$  and  $a_{th} = 4.0$  (Fig. 13).

The interior velocity  $u$  can be determined in the same way. The dimensional velocity in the actively convecting region scales as

$$u = a_u \frac{\kappa}{d_{eff}} \left( \frac{\alpha\rho g\gamma^{-1}d_{eff}^{(n+2)/n}}{b^{1/n}\kappa^{1/n}\exp(-\gamma T_i/n)} \right)^{\beta_u}, \quad (B7)$$

where  $a_u$  and  $\beta_u$  are constants.

In the numerical simulations the rms velocity for the entire layer,  $u_{rms}$ , was determined. The fact that  $u_{rms}$  is negligible in the stagnant lid suggests an approximate relationship between  $u_{rms}$  and the velocity  $u$  in the interior:

$$u = u_{rms} \frac{d}{d_{eff}} = u_{rms}(1 - 2Nu^{-1} + 2a_{th}\theta^{-1})^{1/2}. \quad (B8)$$

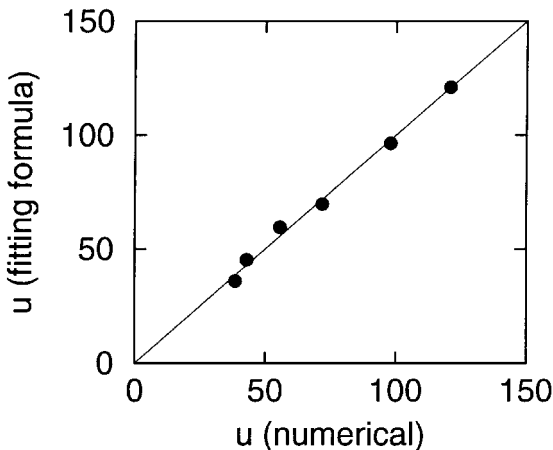


**FIG. 14.** The results of the fit for the rms velocity: the values calculated using the fitting formula (B9) versus the numerical data.

The fitting formula for the measured values of  $u_{rms}$  is then obtained in the same way as for the Nu–Ra relationship:

$$u_{rms} = a_u(1 - 2Nu^{-1} + 2a_{th}\theta^{-1})^{\beta_u(n+2)/2n}\theta^{-\beta_u}Ra_{H,0}^{\beta_u} \times \exp(\beta_u\theta/nNu). \quad (B9)$$

Using the theoretical value of  $\beta_u = 2n/(n+2) = 1.2$ , we obtain  $a_u = 0.050$ .

## ACKNOWLEDGMENTS

The authors thank G. Schubert and D. A. Yuen for constructive reviews which greatly benefited the paper. This work was supported by NASA Grant NAG5-6897, the Alfred P. Sloan Foundation, and the New Mexico Universities Collaborative Research program.

## REFERENCES

- Anderson, D. L. 1980. Tectonics and composition of Venus. *Geophys. Res. Lett.* **7**, 101–102.
- Anderson, D. L. 1989. *Theory of the Earth*. Blackwell Scientific, Boston, MA.
- Arkani-Hamed, J., and M. N. Toksöz 1984. Thermal evolution of Venus. *Phys. Earth Planet. Int.* **34**, 232–250.
- Arkani-Hamed, J., G. G. Schaber, and R. G. Strom 1993. Constraints on the thermal evolution of Venus inferred from Magellan data. *J. Geophys. Res.* **98**, 5309–5315.
- Basilevsky, A. T., J. W. Head, G. G. Schaber, and R. G. Strom 1997. The resurfacing history of Venus. In *Venus II* (S. W. Bougher, D. M. Hunten, and R. J. Phillips, Eds.), pp. 1245–1287. Univ. of Arizona Press, Tucson.
- Brown, C. D., and R. E. Grimm 1997. Tessera deformation and the contemporaneous thermal state of the plateau highlands, Venus. *Earth Planet. Sci. Lett.* **147**, 1–10.
- Bullock, M. A., and D. H. Grinspoon 1996. The stability of climate on Venus. *J. Geophys. Res.* **101**, 7521–7529.
- Bullock, M. A., D. H. Grinspoon, and J. W. Head 1993. Venus resurfacing rates: Constraints provided by 3-D Monte Carlo simulations. *Geophys. Res. Lett.* **20**, 2147–2150.
- Busse, F. H. 1979. High Prandtl number convection. *Phys. Earth. Planet. Int.* **19**, 149–157.
- Carslaw, H. S., and J. C. Jaeger 1959. *Conduction of Heat in Solids*. Oxford Univ. Press, London.
- Chopra, P. N., and M. S. Paterson 1984. The role of water in the deformation of dunite. *J. Geophys. Res.* **89**, 7861–7876.
- Christensen, U. R. 1984. Heat transport by variable viscosity convection and implications for the Earth's thermal evolution. *Phys. Earth Planet. Int.* **35**, 264–282.
- Christensen, U. R. 1985a. Thermal evolution models for the Earth. *J. Geophys. Res.* **90**, 2995–3007.
- Christensen, U. R. 1985b. Heat transfer by variable viscosity convection. II. Pressure influence, non-Newtonian rheology, and decaying heat sources. *Phys. Earth Planet. Inter.* **37**, 183–205.
- Cook, F. A., and D. L. Turcotte 1981. Parameterized convection and the thermal history of the Earth. *Tectonophysics* **75**, 1–17.
- Davaille, A., and C. Jaupart 1993. Transient high Rayleigh number thermal convection with large viscosity variations. *J. Fluid Mech.* **253**, 141–166.
- Doin, M.-P., L. Fleitout, and U. Christensen 1997. Mantle convection and stability of depleted and undepleted continental lithosphere. *J. Geophys. Res.* **102**, 2771–2787.
- Fowler, A. C. 1985. Fast thermoviscous convection. *Stud. Appl. Math.* **72**, 1–34.
- Fowler, A. C. 1993. Boundary layer theory and subduction. *J. Geophys. Res.* **98**, 21997–22005.

- Fowler, A. C., and S. B. G. O'Brien 1996. A mechanism for episodic subduction on Venus. *J. Geophys. Res.* **101**, 4755–4763.
- Grasset, O., and E. M. Parmentier 1998. Thermal convection in a volumetrically heated, infinite Prandtl number fluid with strongly temperature-dependent viscosity: Implications for planetary evolution. *J. Geophys. Res.* **103**, 18171–18181.
- Grimm, R. E., and P. C. Hess 1997. The crust of Venus. In *Venus II* (S. W. Bougher, D. M. Hunten, and R. J. Phillips, Eds.), pp. 1245–1287. Univ. of Arizona Press, Tucson.
- Grimm, R. E., and S. C. Solomon 1988. Viscous relaxation of impact crater relief on Venus: Constraints on crustal thickness and thermal gradient. *J. Geophys. Res.* **93**, 11911–11929.
- Grosfils, E. B., and J. W. Head 1996. The timing of giant radiating dike swarms emplacement on Venus: Implications for resurfacing of the planet and its subsequent evolution. *J. Geophys. Res.* **101**, 4645–4656.
- Hansen, V. L., and J. J. Willis 1996. Structural analysis of a sampling of tesserae: Implications for Venus geodynamics. *Icarus* **23**, 296–312.
- Hansen, V. L., and J. J. Willis 1998. Ribbon terrain formation, southwestern Fortuna Tessera, Venus: Implications for lithosphere evolution. *Icarus* **132**, 321–343.
- Head, J. W., and A. T. Basilevsky 1998. Sequence of tectonic deformation in the history of Venus: Evidence from global stratigraphic relationships. *Geology* **26**, 35–38.
- Head, J. W., L. S. Crumpler, J. C. Aubele, J. E. Guest, and R. S. Saunders 1991. Venus volcanism: Classification of volcanic features and structures, associations, and global distribution from Magellan data. *Science* **252**, 276–288.
- Herrick, R. R. 1994. Resurfacing history of Venus. *Geology* **22**, 703–706.
- Herrick, R. R., and E. M. Parmentier 1994. Episodic large-scale overturn of two-layer mantle in terrestrial planets. *J. Geophys. Res.* **99**, 2053–2062.
- Herrick, R. R., and R. J. Phillips 1994. Implications of a global survey of Venusian impact craters. *Icarus* **111**, 387–416.
- Ito, E., and E. Takahashi 1987. Melting of peridotite at uppermost lower-mantle conditions. *Nature* **328**, 514–517.
- Jarvis, G. T., and W. R. Peltier 1982. Mantle convection as a boundary layer phenomenon. *Geophys. J. R. Astron. Soc.* **68**, 385–424.
- Karato, S.-I. 1989. Grain growth kinetics in olivine aggregates. *Tectonophysics* **168**, 255–273.
- Karato, S.-I., and D. C. Rubie 1997. Toward an experimental study of deep mantle rheology: A new multianvil sample assembly for deformation studies under high pressures and temperatures. *J. Geophys. Res.* **102**, 20111–20122.
- Karato, S.-I., and P. Wu 1993. Rheology of the upper mantle: A synthesis. *Science* **260**, 771–778.
- Karato, S.-I., S. Zhang, and H.-R. Wenk 1995. Superplasticity in the Earth's lower mantle: Evidence from seismic anisotropy and rock physics. *Science* **270**, 458–461.
- Kaula, W. M. 1990a. Venus: A contrast in evolution to Earth. *Science* **247**, 1191–1196.
- Kaula, W. M. 1990b. Mantle convection and crustal evolution on Venus. *Geophys. Res. Lett.* **17**, 1401–1403.
- Kaula, W. M. 1994. Comment on "An episodic hypothesis for Venusian tectonics" by Donald L. Turcotte. *J. Geophys. Res.* **99**, 19095–19096.
- Kaula, W. M. 1995. Venus reconsidered. *Science* **270**, 1460–1464.
- King, S. D. 1995. Models of mantle viscosity. In *Mineral Physics and Crystallography: A Handbook of Physical Constants* (T. J. Ahrens, Ed.), pp. 227–236. AGU, Washington, DC.
- Kohlstedt, D. L., and M. E. Zimmerman 1996. Rheology of partially molten mantle rocks. *Annu. Rev. Earth Planet. Sci.* **24**, 41–62.
- Kucinskis, A. B., and D. L. Turcotte 1994. Isostatic compensation of equatorial highlands on Venus. *Icarus* **112**, 104–116.
- Larsen, T. B., and D. A. Yuen 1997. Fast plumeheads—Temperature-dependent versus non-Newtonian rheology. *Geophys. Res. Lett.* **24**, 1995–1998.
- Larsen, T. B., D. A. Yuen, J. L. Smedsmo, and A. V. Malevsky 1996. Thermo-mechanical modeling of pulsation tectonics and consequences on lithospheric dynamics. *Geophys. Res. Lett.* **23**, 217–220.
- Larsen, T. B., D. A. Yuen, J. L. Smedsmo, and A. V. Malevsky 1997. Generation of fast time scale phenomena in thermomechanical processes. *Phys. Earth Planet. Int.* **102**, 213–222.
- Li, P., S. Karato, and Z. Wang 1996. High-temperature creep in fine-grained polycrystalline CaTiO<sub>3</sub>, an analogue material of (Mg,Fe)SiO<sub>3</sub>. *Phys. Earth Planet. Inter.* **95**, 19–366.
- Mackwell, S. J., M. E. Zimmerman, and D. L. Kohlstedt 1998. High temperature deformation of dry diabase with application to tectonics on Venus. *J. Geophys. Res.* **103**, 975–984.
- McKenzie, D. 1984. The generation and compaction of partially molten rock. *J. Petrology* **5**, 713–765.
- McKenzie, D. 1994. The relationship between topography and gravity on Earth and Venus. *Icarus* **112**, 55–88.
- McKenzie, D., and M. J. Bickle 1988. The volume and composition of melt generated by extension of the lithosphere. *J. Petrol.* **29**, 625–679.
- McKenzie, D. P., and N. Weiss 1975. Speculations on the thermal and tectonic history of the earth. *Geophys. J. R. Astron. Soc.* **42**, 131–174.
- McKinnon, W. B., K. Zahnle, B. A. Ivanov, and H. J. Melosh 1997. Cratering on Venus: Modeling and observations. In *Venus II* (S. W. Bougher, D. M. Hunten, and R. J. Phillips, Eds.), pp. 969–1014. Univ. of Arizona Press, Tucson.
- Moore, D. R., and N. O. Weiss 1973. Two-dimensional Rayleigh-Bénard convection. *J. Fluid Mech.* **58**, 289–312.
- Moore, W. B., and G. Schubert 1997. Venusian crustal and lithospheric properties from nonlinear regressions of highland geoid and topography. *Icarus* **128**, 415–428.
- Moresi, L.-N., and V. S. Solomatov 1995. Numerical investigation of 2D convection with extremely large viscosity variations. *Phys. Fluid* **7**, 2154–2162.
- Moresi, L.-N., and V. S. Solomatov 1998. Mantle convection with a brittle lithosphere: Thoughts on the global tectonic style of the Earth and Venus. *Geophys. J.* **133**, 669–682.
- Morris, S., and D. Canright 1984. A boundary layer analysis of Bénard convection in a fluid of strongly temperature dependent viscosity. *Phys. Earth Planet. Int.* **36**, 355–373.
- Namiki, N., and S. C. Solomon 1993. The gabbro-eclogite phase transition and the elevation of mountain belts on Venus. *J. Geophys. Res.* **98**, 15025–15031.
- Namiki, N., and S. C. Solomon 1994. Impact crater densities on volcanoes and coronae on Venus: Implications for volcanic resurfacing. *Science* **265**, 929–933.
- Namiki, N., and S. C. Solomon 1998. Volcanic degassing of argon and helium and the history of crustal production on Venus. *J. Geophys. Res.* **103**, 3655–3677.
- Nimmo, F., and D. McKenzie 1996. Modeling plume-related uplift, gravity and melting on Venus. *Earth Planet. Sci. Lett.* **145**, 109–123.
- Nimmo, F., and D. McKenzie 1998. Volcanism and tectonics on Venus. *Annu. Rev. Earth Planet. Sci.* **26**, 23–51.
- Ogawa, M., G. Schubert, and A. Zebib 1991. Numerical simulations of three-dimensional thermal convection in a fluid with strongly temperature-dependent viscosity. *J. Fluid Mech.* **233**, 299–328.
- O'Nions, R. K., N. M. Evensen, and P. J. Hamilton 1979. Geochemical modeling of mantle differentiation and crustal growth. *J. Geophys. Res.* **84**, 6091–6101.
- Parmentier, E. M., and P. C. Hess 1992. Chemical differentiation of a convecting planetary interior: Consequences for a one plate planet such as Venus. *Geophys. Res. Lett.* **19**, 2015–2018.
- Phillips, R. J. 1990. Convection-driven tectonics on Venus. *J. Geophys. Res.* **95**, 1301–1316.
- Phillips, R. J. 1994. Estimating lithospheric properties at Atla Regio, Venus. *Icarus* **112**, 147–170.

- Phillips, R. J., and R. E. Grimm 1990. Generation of basaltic crust on Venus. *Proc. Lunar Planet. Sci. Conf. 21st*, 1021–1022.
- Phillips, R. J., and V. L. Hansen 1994. Tectonic and magmatic evolution of Venus. *Annu. Rev. Earth Planet. Sci.* **22**, 597–654.
- Phillips, R. J., and V. L. Hansen 1998. Geological evolution of Venus: Rises, plains, plumes, and plateaus. *Science* **279**, 1492–1497.
- Phillips, R. J., W. M. Kaula, G. E. McGill, and M. C. Malin 1981. Tectonics and evolution of Venus. *Science* **212**, 879–887.
- Phillips, R. J., R. F. Raubertas, R. E. Arvidson, I. C. Sarkar, R. R. Herrick, N. Izenberg, and R. E. Grimm 1992. Impact craters and Venus resurfacing history. *J. Geophys. Res.* **97**, 15923–15948.
- Price, M., and J. Suppe 1994. Mean age of rifting and volcanism on Venus deduced from impact crater densities. *Nature* **372**, 756–759.
- Price, M. H., G. Watson, J. Suppe, and C. Brankman 1996. Dating volcanism and rifting on Venus using impact crater densities. *J. Geophys. Res.* **101**, 4657–4671.
- Ratcliff, J. T., P. J. Tackley, G. Schubert, and A. Zebib 1997. Transitions in thermal convection with strongly variable viscosity. *Phys. Earth Planet. Int.* **102**, 201–212.
- Reese, C. C., V. S. Solomatov, and L.-N. Moresi 1998. Heat transport efficiency for stagnant lid convection with dislocation viscosity: Application to Venus and Mars. *J. Geophys. Res.* **103**, 13643–13658.
- Scarfe, C. M., and E. Takahashi 1986. Melting of garnet peridotite to 13 GPa and the early history of the upper mantle. *Nature* **322**, 354–356.
- Schaber, G. G., R. G. Strom, H. J. Moore, L. A. Soderblom, R. L. Kirk, D. J. Dawson, L. R. Gaddis, J. M. Boyce, and J. Russell 1992. Geology and distribution of impact craters on Venus: What are they telling us? *J. Geophys. Res.* **97**, 13256–13301.
- Schubert, G., and D. T. Sandwell 1995. A global survey of possible subduction sites on Venus. *Icarus* **117**, 173–196.
- Schubert, G., P. Cassen, and R. E. Young 1979. Subsidiary convective cooling histories of the terrestrial planets. *Icarus* **38**, 192–211.
- Schubert, G., V. S. Solomatov, P. J. Tackley, and D. L. Turcotte 1997. Mantle convection and the thermal evolution of Venus. In *Venus II* (S. W. Bougher, D. M. Hunten, and R. J. Phillips, Eds.), pp. 1245–1287. Univ. of Arizona Press, Tucson.
- Schubert, G., S. C. Solomon, D. L. Turcotte, M. J. Drake, and N. H. Sleep 1992. Origin and thermal evolution of Mars. In *Mars* (H. H. Kieffer, B. M. Jakosky, C. W. Snyder, and M. S. Matthews, Eds.), pp. 147–183. Univ. of Arizona Press, Tucson.
- Sharpe, H. N., and W. R. Peltier 1979. A thermal history for the Earth with parameterized convection. *Geophys. J. R. Astron. Soc.* **59**, 171–203.
- Simons, M., S. C. Solomon, and B. H. Hager 1997. Localization of gravity and topography: Constraints on the tectonics and mantle dynamics of Venus. *Geophys. J. Int.* **131**, 24–44.
- Smrekar, S. E. 1994. Evidence for active hotspots on Venus from analysis of Magellan gravity data. *Icarus* **112**, 2–26.
- Smrekar, S. E., and E. M. Parmentier 1996. The interaction of mantle plumes with surface thermal and chemical boundary layers: Application to hotspots on Venus. *J. Geophys. Res.* **101**, 5397–5410.
- Smrekar, S. E., W. S. Kiefer, and E. R. Stefan 1997. Large volcanic rises on Venus. In *Venus II* (S. W. Bougher, D. M. Hunten, and R. J. Phillips, Eds.), pp. 845–878. Univ. of Arizona Press, Tucson.
- Solomatov V. S. 1993. Parameterization of temperature- and stress-dependent viscosity convection and the thermal evolution of Venus. In *Flow and Creep in the Solar System: Observations, Modeling and Theory* (D. B. Stone and S. K. Runcorn, Eds.), pp. 131–145. Kluwer, Netherlands.
- Solomatov, V. S. 1995. Scaling of temperature- and stress-dependent viscosity convection. *Phys. Fluids* **7**, 266–274.
- Solomatov, V. S. 1996. Can hotter mantle have a larger viscosity? *Geophys. Res. Lett.* **23**, 937–940.
- Solomatov, V. S., and L.-N. Moresi 1996. Stagnant lid convection on Venus. *J. Geophys. Res.* **101**, 4737–4753.
- Solomatov, V. S., and L.-N. Moresi 1997. Three regimes of mantle convection with non-Newtonian viscosity and stagnant lid convection on the terrestrial planets. *Geophys. Res. Lett.* **24**, 1907–1910.
- Solomatov, V. S., and D. J. Stevenson 1993. Nonfractional crystallization of a terrestrial magma ocean. *J. Geophys. Res.* **98**, 5391–5406.
- Solomon, S. C., M. A. Bullock, and D. H. Grinspoon 1998. Climate change as a regulator of global tectonics on Venus. *Lunar and Planetary Science 29th Abstract* 1624.
- Spohn, T. 1991. Mantle differentiation and thermal evolution of Mars, Mercury, and Venus. *Icarus* **90**, 222–236.
- Spohn, T., and G. Schubert 1982. Models of mantle convection and the removal of heat from the Earth's interior. *J. Geophys. Res.* **87**, 4682–4696.
- Steinbach, V., and D. A. Yuen 1992. The effects of multiple phase transitions on Venusian mantle convection. *Geophys. Res. Lett.* **19**, 2243–2246.
- Stengel, K. C., D. C. Oliver, and J. R. Booker 1982. Onset of convection in a variable viscosity fluid. *J. Fluid. Mech.* **120**, 411–431.
- Stevenson, D. J., and J. S. Turner 1979. Fluid models of mantle convection. In *The Earth, Its Origin, Structure, and Evolution* (M. McElhinny, Ed.), pp. 227–263. Academic Press, New York.
- Stevenson, D. J., T. Spohn, and G. Schubert 1983. Magnetism and thermal evolution of the terrestrial planets. *Icarus* **54**, 466–489.
- Tackley, P. J. 1993. Effects of strongly temperature-dependent viscosity on time-dependent, three-dimensional models of mantle convection. *Geophys. Res. Lett.* **20**, 2187–2190.
- Tackley, P. J., and D. J. Stevenson 1993. A mechanism for spontaneous self-perpetuating volcanism on the terrestrial planets. In *Flow and Creep in the Solar System: Observations, Modeling and Theory* (D. B. Stone and S. K. Runcorn, Eds.), pp. 307–321. Kluwer, Netherlands.
- Taylor, S. R. 1989. Growth of planetary crusts. *Tectonophysics* **161**, 147–156.
- Trompert, R. A., and U. Hansen 1998. On the Rayleigh number dependence of convection with a strongly temperature-dependent viscosity. *Phys. Fluids* **10**, 351–360.
- Turcotte, D. L. 1993. An episodic hypothesis for Venusian tectonics. *J. Geophys. Res.* **98**, 17061–17068.
- Turcotte, D. L. 1996. Magellan and comparative planetology. *J. Geophys. Res.* **101**, 4765–4773.
- Turcotte, D. L., and E. R. Oxburgh 1967. Finite amplitude convection cells and continental drift. *J. Fluid Mech.* **28**, 29–42.
- Turcotte, D. L., F. A. Cooke, and R. J. Willeman 1979. Parameterized convection within the moon and the terrestrial planets. *Proc. 10th Lunar Planet. Sci. Conf.* 2375–2392.
- van den Berg, A. P., and D. A. Yuen 1997. Is the lower mantle rheology Newtonian today? *Geophys. Res. Lett.* **23**, 2033–2036.
- Weinstein, S. A. 1996. The potential role of non-Newtonian rheology in the resurfacing of Venus. *Geophys. Res. Lett.* **23**, 511–514.
- Watson, S., and D. McKenzie 1991. Melt generation by plumes: A study of Hawaiian volcanism. *J. Petrol.* **32**, 501–537.
- Zharkov, V. N., and V. S. Solomatov 1992. Models of thermal evolution of Venus. In *Venus Geology, Geochemistry and Geophysics*. (V. L. Barsukov et al., Eds.), pp. 280–319. Univ. of Ariz. Press, Tucson.